Positions of the Glycans in Molluscan Hemocyanin, Determined by Fluorescence Spectroscopy

ARTICLE *in* JOURNAL OF FLUORESCENCE · MARCH 2013

Impact Factor: 1.93 · DOI: 10.1007/s10895-013-1171-4 · Source: PubMed

6 AUTHORS, INCLUDING:

Pavlina Dolashka
Bulgarian Academy of Sciences
111 PUBLICATIONS **912** CITATIONS
SEE PROFILE

Lyudmila Velkova
Bulgarian Academy of Sciences
20 PUBLICATIONS **145** CITATIONS
SEE PROFILE

Aleksandar Dolashki
Bulgarian Academy of Sciences
17 PUBLICATIONS **116** CITATIONS
SEE PROFILE

Wolfgang Voelter
University of Tuebingen
941 PUBLICATIONS **11,469** CITATIONS
SEE PROFILE

J Fluoresc (2013) 23:753–760
DOI 10.1007/s10895-013-1171-4

ORIGINAL PAPER

Positions of the Glycans in Molluscan Hemocyanin, Determined by Fluorescence Spectroscopy

Elena Kostadinova · Pavlina Dolashka · Lyudmila Velkova · Aleksandar Dolashki · Stefan Stevanovic · Wolfgang Voelter

Received: 16 November 2012 / Accepted: 31 January 2013 / Published online: 15 March 2013

Abstract Molluscan hemocyanins are glycoproteins with different quaternary and carbohydrate structures. It was suggested that the carbohydrate chains of some Hcs are involved in their antiviral and antitumor effect, as well in the organization of the quaternary structure of the molecules. Using a well-known complex for saccharide sensing, positions and access to the carbohydrate chains in the native hemocyanins from *Rapana venosa* (RvH) and *Helix lucorum* (HlH) and also their structural subunits (RvH1, RvH2 and β_cHlH) and functional units (FUs) were analysed by fluorescence spectroscopy and circular dichroism. Almost no effect was observed in the fluorescence emission after titration of the complex with native RvH and HlH due to lack of free hydroxyl groups which are buried in the didecameric form of the molecules. Titration with the structural subunits β_cHlH and RvH2, increasing of the emission indicates the presence of free hydroxyl groups compared to the native molecules. Complex titration with the structural subunit βc-HlH of *H. lucorum* Hcs leads to a 2.5 fold increase in fluorescence intensity. However, the highest emission was measured after titration of the complex with FU βcHlH-g. The result was explained by the structural model of β_cHlH-g showing the putative position of the glycans on the surface of the molecule. The results of the fluorescent measurements are in good correlation with those of the circular dichroism data, applied to analyse the effect of titration on the secondary structure of the native molecules and functional units. The results also support our previously made suggestion that the N-linked oligosaccharide trees are involved in the quaternary organization of molluscan Hcs.

Keywords Hemocyanins · Glycans · Fluorescence spectroscopy and circular dichroism

E. Kostadinova · P. Dolashka (✉) · L. Velkova · A. Dolashki · S. Stevanovic
Institute of Organic Chemistry, Bulgarian Academy of Sciences, G. Bonchev 9, 1113 Sofia, Bulgaria
e-mail: pda54@abv.bg

P. Dolashka
e-mail: dolashka@orgchm.bas.bg

W. Voelter
Interfacultary Institute of Biochemistry, University of Tubingen, Hoppe-Seyler-Strasse 4, 72076 Tubingen, Germany

S. Stevanovic
Institute for Cell Biology, Department of Immunology, University of Tübingen, D-72076 Tübingen, Germany

Introduction

Hemocyanins (Hcs) are oxygen-transporting proteins, freely dissolved in the hemolymph of several arthropods and molluscs [1, 2]. Molluscan hemocyanins are glycoproteins with high molecular masses and complicated quaternary and oligosaccharide structures. They have been intensively studied for their function, evolution [1–3] and for their immunological and clinical applications [2–4]. Molluscan hemocyanins have different quaternary structure and occur either as decamers (five subunit dimers assembled as a hollow cylinder), didecamers (face-to-face assembly of two decamers), or multidecamers (elongated cylinders formed from a didecamer with added decamers) [1, 5]. The oligomers consist of several 11S basic structural units with molecular masses ranging between 220 and 400 kDa. Each structural subunit is organized by seven or eight globular functional

units (FUs) of approximately 50 kDa and each contains one dioxygen-binding Cu(I) pair [6–8].

Beside the differences in the quaternary structure of the arthropodan and molluscan Hcs, they also differ in their carbohydrate content and monosaccharide composition. The carbohydrate content of the arthropodan Hcs is relatively low (0.1–2 %, w/w) [9], while in the molluscan Hcs it is usually higher (2–9 %, w/w) containing also unusual monosaccharides [10–13]. The oligosaccharide structures of molluscan hemocyanins of *Helix pomatia* (HpH) [14], *Lymnaea stagnalis* [15], *Rapana venosa* (RvH) [11–13], and keyhole limpet *Megathura crenulata* (KLH) [16] were studied and it was found that they are heterogeneously glycosylated proteins, carrying mainly high mannose-type glycans with 5–7 mannosyl residues, hybrid-type species with five mannoses and one N-acetylgalactosamine-containing chain, as well as truncated sugar chains derived thereof. The carbohydrate moiety of molluscan Hcs has recently received particular interest because of its immunostimulatory properties [17–20] and is used in clinical studies due to these properties. It was found that the Hcs of KLH1 [20, 21], *Helix vulgaris* (HvH) [22], *Concholepas concholepas* (CcH) [23] and *R. venosa* [24–26] have significant antitumor activities, and can be used as immunotherapeutic agents in the treatment of certain types of cancer (mainly bladder carcinoma), as well as carriers for vaccines [27–29]. It was also suggested that the carbohydrate chains of some FUs of *R. venosa* Hcs are involved in their antiviral effect against the herpes simplex virus (HSV) type 1 and respiratory syncytial virus (RSV) [30]. Moreover, in our previous work we suggested another function of the carbohydrate chains in the molluscan Hcs. We assumed that they are involved in the organization of the quaternary structure of the molecules of Hcs and the individual polypeptides of the different FUs are also linked to each other in a network generated by oligosaccharides [31].

The aim of the present study is to confirm this suggestion by identification of the positions and the accessibility of the carbohydrate chains in the native, structural subunits and functional units of hemocyanins from *R. venosa* and *H. lucorum*, using the well-known complex for saccharide sensing in combination with the very sensitive fluorescence spectroscopy method.

Both hemocyanins, RvH and HlH, were chosen for analysis because they differ in their structure. Native RvH is organized by two structural subunits RvH1 and RvH2 with molecular masses of 420 and 400 kDa, respectively [32, 33]. In contrast, the hemocyanin of the garden snail *H. lucorum* is organized by three different isopolypeptides which were isolated from the hemolymph and named as β-HlH, α_D-HlH, and α_N-HlH structural subunits. Each structural subunit contains 8 functional units (FU) with masses of about 50–60 kDa [31]. Both hemocyanins, RvH and HlH, differ not only in their quaternary structure, but also in their oligosaccharide structures.

Materials and Methods

Isolation of the Native Hemocyanins and their Isoforms

Rapana venosa hemocyanin was isolated from Black Sea marine snails as already described [32]. The dissociation of native Hc was achieved by dialyzing the native protein against a 0.13 M glycine/NaOH bufer, pH9.6, and the structural subunits RvH1 and RvH2 were purified by means of ion-exchanging chromatography on a Resource Q (Pharmacia) column of 6 ml using an FPLC separation system. Elution was performed as described by Dolashka-Angelova et al [32].. The native molecule of *H. lucorum* hemolymph was collected from the foot of the garden snails (25 g), centrifuged at 1000 g and 4 °C for 20 min for removal of rough particles. Hemocyanin was isolated as already described by Velkova et al. [33].

Fluorescence Measurements

Fluorescence measurements were carried out on a spectrofluorimeter Jasco FP-6600. For our purposes we used a two-component sensing system comprising an anionic fluorescent dye and N,N'-bis-(benzyl-2-boronic acid)-[4,4′]bipyridinium dibromide (*o*-BBV) serving as fluorescence quencher and saccharide receptor [34–38]. After formation of the complex titration with the tested samples was performed. The measurements were carried out between 460 and 650 nm, with excitation wavelength at 460 nm in a 1 cm quartz cuvette upon addition of 10 μl samples with different concentrations: RvH− 0÷0.14 mg/ml; RvH2− 0÷0.5 mg/ml; HlH− 0÷0.12 mg/ml; βc-HlH− 0÷0.38 mg/ml and βc-HlH-g 0÷0.52 mg/ml. All studies were carried out in 10 mM Tris buffer, pH7.4, under ambient conditions (25 °C, in air).

CD Measurements

Circular dichroism (CD) spectra were recorded on a J-720 dichrograph (Jasco, Tokyo, Japan). Round quartz cells with a path length of 10 mm were used in all experiments. CD spectra were recorded in the range between 200 and 250 nm with a band width of 1 nm, a scan speed of 50 nm/min, a time constant of 8.0 s and accumulation −4. The hemocyanin solutions with A_{280}=0,215 were prepared in 10 mM Tris buffer (pH7.4). The concentration of the titrating agent (*o*-BBV) varies from 0 to1.2×10^{-4}M.

Identification of FUs

The obtained fraction after treatment of the structural subunit βc-HlH with tripsyn (1:400) was further purified by HPLC using a Nucleosil 100 RP-18 column (250 mm 10 mm; 7 m; Macherey-Nagel, Germany). For elution, a

linear gradient from 5 % solvent A (0.1 % TFA in water) to 100 % solvent B (0.085 % TFA in acetonitrile) within 70 min, at a flow rate of 1 ml/min, was used. The HPLC fractions were detected at a wavelength of 278 nm and then collected. Isolated HPLC fractions were dried and after dissolving them in 40 % methanol/1 % formic acid, were subjected to automated Edman N-terminal sequencing on a Pulsed Liquid Protein Sequencer (Applied Biosystems GmbH, Foster City, CA). Alignments of the obtained N-terminal amino acid sequences of FUs of βc-HlH were created by LALINGS.

A 3D model of βcHlH-g was created by using the Swiss PDB viewer and the model of functional unit "g" from *Octopus dofleini* (OdH-g) hemocyanin.

Results and Discussion

Several aspects of the structural–functional peculiarities of the Hcs make them important materials to address relevant problems of structural biology including molecular recognition among subunits, protein–water interactions or allosteric regulation [39, 40]. In this study, two different hemocyanins from *R. venosa* and *H. lucorum*, with different and well-known structures were used for the investigation.

Fluorescence Analysis of Molluscan Hcs After Titration with the Complex

Fluorescence spectroscopy and circular dichroism are very sensitive and useful methods to analyse proteins [41–44]. Therefore, in the present work, we present the analyses of native hemocyanins with different carbohydrate structure including their isoforms, using fluorescence spectroscopy and circular dichroism. To analyse the function and position of the glycans in the native molecules and different isoforms of Hcs from Rapana and Helix, a solution of pyranine and *o*-BBV (complex) was titrated with different concentrations of the samples and analysed by fluorescence spectroscopy as a very sensitive method. This complex was previously described and used only for analyses of simple carbohydrates. However, we have investigated the sensitivity of the complex to analyze more complicated carbohydrate structures like cyclodextrins, molluscan and arthropodan hemocyanins and the previous results confirmed that it is suitable for this purpose [45].

The proposed mechanism for the complex is that the electrostatic association of pyranine and the quencher results in "ground-state complex formation", facilitating electron transfer from the dye to the viologen, which leads to a decrease in fluorescence intensity [38]. When different saccharides are added to the system, formation of two anionic boronate esters effectively neutralize the dicationic viologen, thus greatly diminishing its quenching efficiency, and an increase in the fluorescence intensity of the dye is observed. Fluorescence modulation is therefore directly correlated with saccharide concentration.

After titration of solution of pyranine (1.33×10^{-6}) in 50 mM phosphate buffer, pH7.5, with increasing amounts of *o*-BBV, a 4-fold decrease in the fluorescence emission of pyranine was observed.(λ_{em}=508 nm, λ_{ex}=460 nm) (not shown).

The complex was titrated with native *R. venosa* hemocyanin and its isoforms because the carbohydrate structure and the linkage sites of RvH were very well analysed using different approaches [11–13]. A highly heterogeneous mixture of glycans with compositions Hex_{0-9} $HexNAc_{2-4}$ Hex_{0-3} $Pent_{0-3}$ Fuc_{0-3} was analysed by MALDI-TOF-MS and tandem mass spectrometry on a Q-Trap mass spectrometer after enzymatic liberation of the N-glycans from the polypeptides. A novel type of N-glycan, with an internal fucose residue connecting one GalNAc(β1−2) and one hexuronic acid, was detected only in both subunits of RvH [12, 13]. Results on the titration of the complex with native RvH and one of its subunits (RvH2), respectively are shown in Fig. 1a. Titration of the complex with increasing RvH concentrations leads to minimal increase (5 a.u) in fluorescence intensity, since obviously few interaction is possible between carbohydrate moieties and the cationic viologen. On

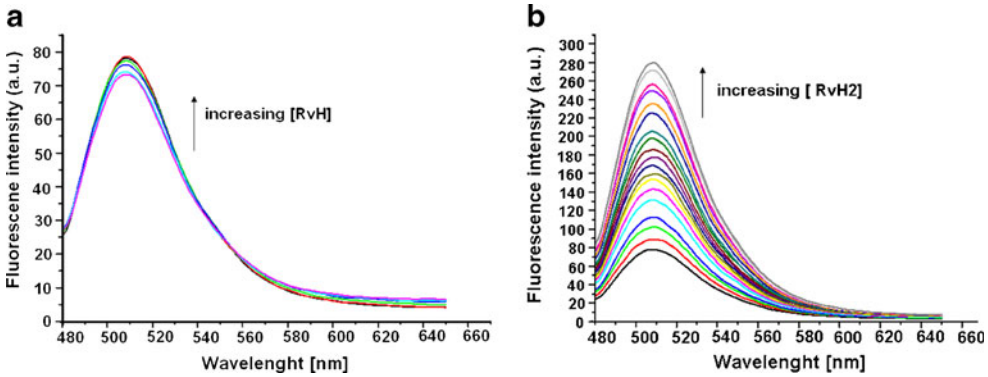

Fig. 1 **a** Fluorescence emission spectra of the complex pyranine (1.33×10^{-6}M) in presence of *o*-BBV upon addition with increasing concentrations of RvH (0÷0.25 mg/ml). **b** Fluorescence emission spectra of the complex pyranine (1.33×10^{-6}M) in presence of *o*-BBV upon addition with increasing concentrations of RvH2 (0÷0.55 mg/ml)

the other hand, titration with subunit RvH2 leads to 3,5 fold increase in fluorescence intensity confirming that more hydroxyl groups are accessible to the *o*-BBV complex (Fig. 1b). However, the observed increase in emission (205 a.u) is smaller than that obtained in our previous study for the functional unit RvH1-a (280 a.u) [46].

Complex titration was repeated with another molluscan Hc from *H. lucorum*, organized by three structural subunits and differing in oligisacchiride structure. Several core-fucosylated carbohydrate chains, with high degree of methylation were identified in β-HlH. Highly methylated complex structures were also recognized in many glycan structures of gastropod hemocyanins, which suggests that the methylation of N-glycans is very important feature in these organisms [45]. Structural subunit and functional units were isolated as described by Velkova et al. 2010 [33]. To identify the FU, its (VPGDSVRKNVNDL) N-terminal sequence was determined by Edman degradation. From the alignment of the obtained N-terminal sequence with the full sequence of β_cHlH (Table 1) follows that the isolated fraction corresponds to FU β_cHlH-g.

The complex (see above) was titrated with native HlH, its structural subunit β_cHlH and one functional unit β_cHlH-g. A small change in fluorescence intensity (14 a.u) during titration of the complex with different concentrations of the native HlH is observed (Fig. 2a). This result observed for the titration of the complex with native hemocyanin from HlH is in analogy to those recorded for the native Hcs from Rapana and Helix. As mentioned above we assume that these results are due to the lack of free hydroxyl groups, accessible for the boronic acid-appended cationic viologen, which serves as a fluorescence quencher and a saccharide receptor. Hemocyanins are glycoproteins with about 9 % of carbohydrate structure. Therefore they contain large amount of free hydroxyl groups and the lack of the groups is due to the organization of molecule. The native molecule is constituted by two decamers, each arranged by ten glycosylated structural subunits which contain between 7 and 10 carbohydrate chains. The observed very low titration effect of the native molecule of HlH indicates that the glycans are buried or involved in the organization of the macromolecular structure and free hydroxyl groups are not accessible. This suggestion is supported by the results observed after titration of the complex with the isoform βc-HlH of *H. lucorum* Hcs leading to 1.5 fold increase in the fluorescence intensity, which is lower compared to the effect found for RvH2 (Fig. 2b) and one FU of HlH.

The isoform β_c-HlH consists of eight functional units with molecular masses about 50 kDa. During titration of the complex (see above) with one of these functional units, which we identified by N-terminal sequencing as β_cHlH-g, the emission increased to 270 a.u. or about 4-fold (Fig. 2c).

Comparison on the results after titration of the complex with the native molecule of RvH and HlH, as well their isoforms (Fig. 3) show very low effect of the native molecules of both Hcs and more exposed and accessible of the glycans in structural subunit RvH2 than in β_cHlH. Highest emission was measured after titration of the complex with functional unit βcHlH-g which contains only one carbohydrate chain in the contrary to the native molecule and structural subunits. The observed data confirm that using the complex a presence or deficiency of free hydroxyl groups could be identified.

A structural model of functional unit β_cHlH-g, derived from the model of functional unit "g" from *Octopus dofleini* (OdH-g) hemocyanin [47] (Fig. 4) gives the results of the titration experiments a more plausible background. As is shown on Fig. 4, the glycans and the putative glycosylated

Table 1 Alignment of N-terminal sequences of isolated FUs of β_c-HlH

```
β-HlH_a  : --------------VRKNVDKLTKDELYDLQRALRDVVADHSEKGYDEIASFHGYPAKCKH--GDHDVACCVHGD
β-HlH_b  : ----HEHEFHEGVSVRKNVDRLTVEEVAEIREALEKFQNDRSVDGYQAIAEFHGDPGKCPSPTARDRLACCVHGM
β-HlH_c  : ----------TESRLRKEVDHLTAEETLELRHALTALEDDKTLGGYQTLGRYHGSTLWCPSPDAQKKVACCLHGM
β-HlH_d  : YGQEYRPLVTAGSHVRHNLEHLSAGEVESLRSAFLAIQEDHS---YENIAAYHGKPGLCEFEG--RKVACCVHGS
β-HlH_e  : ------HGDRAPLLVRKNVRSLSPLENYHLVKALSSLNADGSADGFQSIATFHAIPPLCPSPTASVRHACCIHGG
β-HlH_f  : --------KVPLNKIRRNIDSLEERDIQSLQTALHDLQEDDSNNGWANLASFHGAPARCPDPE-HPKVACCQHGM
β-HlH_g  : ---------VPGDSVRKNVNDLTDSEVANLRAALRDVQADDGANGFASIAGFHGSPAHCEHDH--HPVACCLHGM
β-HlH_h  : ----------SSNLVRKSVNSLTLGEASNLKQALRELQADHGPGGFEAIAGFHGYPFLCPEKS-DTKYACCVHGM

β-HlH_g : GFPRWHRLYVKQWEDALIAHGSKNGIPYWDWTQSFTELPTLVTQVEDNPFHHGKIDKDH
β-HlH_g : NTTRSPRPQLFSDPASGDESFFYRQVLLAFEQTDYCDFEVQFEFAHNAIHSWTGGKSPY
β-HlH_g : GMSTLEYTAYDPLFLVHHSNVDRQFAIWQALQKFRGLPYNSANCAIQLLHQPMRPFSDS
β-HlH_g : DNVNPTTRAHSTASEAFNYEQLHYHYDNLNFHGDTISQLVNVIDERKSHDRIFAEFLLH
β-HlH_g : SIGTSADVTFELCDEHNHCEFAGTFAILGGPLEMAWSTDRLFRYDVTDVFEKLHLQADS
β-HlH_g : EYHFVDHIVAVNGTELDSHLIKPPSVRFVPGTKVPQAEQAATTYQ.....
```

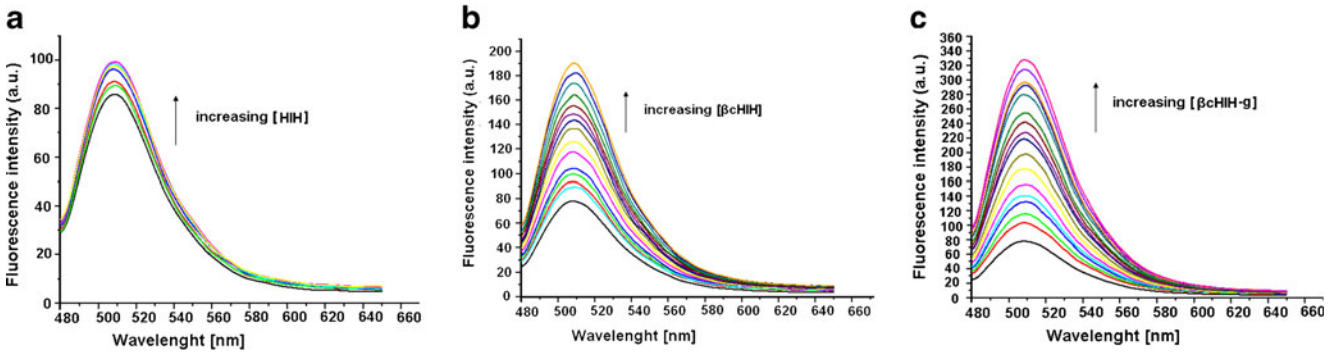

Fig. 2 **a** Fluorescence emission spectra of the complex pyranine (1.33×10^{-6}M) in presence of *o*-BBV upon addition of native Hc from *Helix lucorum* with increasing concentrations (0÷0.33 mg/ml); **b** Fluorescence emission spectra of the complex pyranine (1.33×10^{-6}M) in presence of *o*-BBV upon addition of βc-HlH with increasing concentrations (0÷0.55 mg/ml); **c** Fluorescence emission spectra of the complex pyranine (1.33×10^{-6}M) in presence of *o*-BBV upon addition of βc-HlH-g with increasing concentrations (0÷0.55 mg/ml)

sites N125 and N245 are exposed on the surface in both domains of FU. From the model we may suggest that the putative glycosylation sites are located on the surface of the functional unit, and the carbohydrate chains are easily accessible for the complex resulting in 4-fold increase of the fluorescence intensity (Fig. 2c). However eight FUs fold into structural subunits and some of the hydroxyl group of the monosacchirides of the glycan are buried or involved in the Van der Wals or hydrogenic interactions causing the observed decrease in fluorescence intensity.

Analysis of the secondary structure of Hcs after titration with the complex by CD measurements

The phenomenon of circular dichroism is very sensitive to the secondary structure of proteins. Therefore it was applied to analyse the effect of titration on the secondary structure of the native molecules and functional unit. Circular dichroism spectra of β_cHlH, observed after addition of *o*-BBV with increasing concentration (0; 2.5×10^{-5}M; 5×10^{-5}M; 7.5×10^{-5}M; 1×10^{-4}M; 1.25×10^{-4}M) are shown on Fig. 5a. Very slow unfolding of the investigated β_cHlH was observed after titration with concentration of *o*-BBV from $2{,}5\times10^{-5}$ to 7.5×10^{-5}M. Increasing concentrations of the complex caused a gradual shift from β-sheet to α-helix structure. At the highest concentration of *o*-BBV (1.25×10^{-4}M) only α-helix structure was measured (Fig. 5a, line 6).

According to obtained CD spectra (Fig. 5a), the used hemocyanin, α-helix fraction rapidly decreases for more β-sheets fraction and finally to a random coil structure. Hence, for 0 M of the complex, the protein obvious α-helix characteristics are indicated by a large negative n-<PI> * transition around 222 nm and its <PI> - <PI> * transition which is split into two transitions, a negative band around 208 nm and a positive band around 192 nm (not shown). This phenomenon is characteristic of predominance

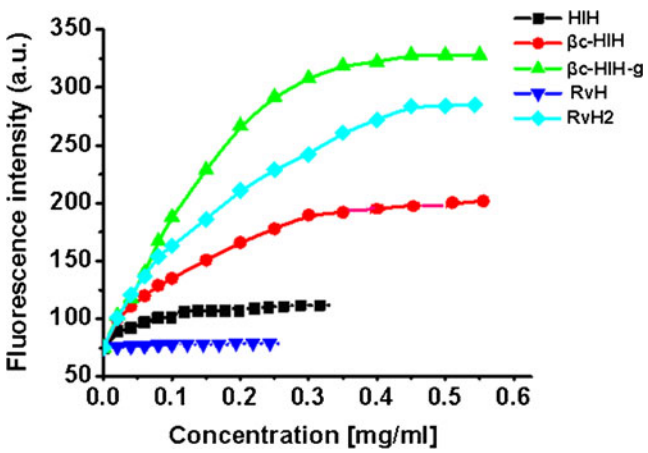

Fig. 3 Relationship between concentration and fluorescence intensity of the tested samples (HlH, βcHlH, βcHlH-g, RvH and RvH2). Concentrations (0÷0.33 mg/ml; 0÷0.55 mg/ml;0÷0.55 mg/ml; 0÷0.25 mg/ml; 0÷0.55 mg/ml)

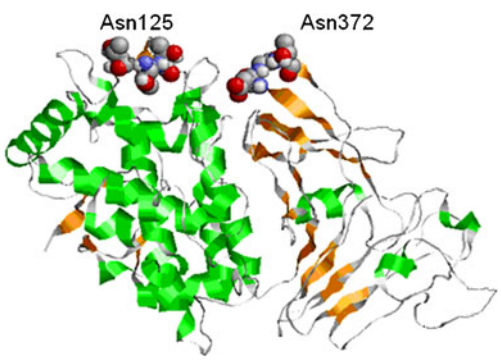

Fig. 4 3D model of βcHlH-g created by using the Swiss PDB viewer and the model of functional unit "g" from *Octopus dofleini* (OdH-g) hemocyanin. Glycans and the putative glycosilated sites N125 and N245 are represent as *balls*

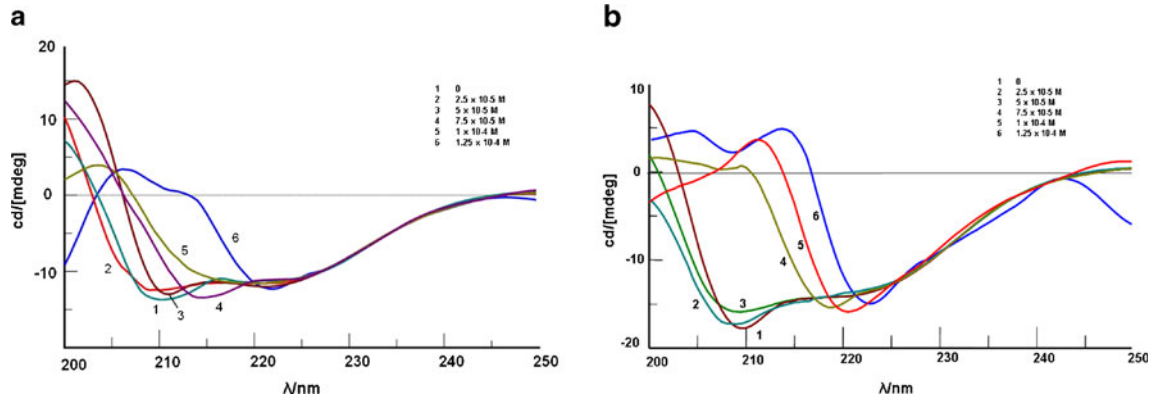

Fig. 5 **a** Circular dichroism spectra of βc-HlH upon addition of *o*-BBV with increasing concentration (0; 2.5×10^{-5}M; 5×10^{-5}M; 7.5×10^{-5}M; 1×10^{-4}M; 1.25×10^{-4}M). **b** Circular dichroism spectra of βc-HlH-g upon addition of *o*-BBV with increasing concentration (0; 2.5×10^{-5}M; 5×10^{-5}M; 7.5×10^{-5}M; 1×10^{-4}M; 1.25×10^{-4}M)

of β-sheets fraction in the protein secondary structure, corresponding to <PI> - <PI> * transition splits into a negative band around 218 nm and a positive one around 195 nm (not shown). The observed spectrum with a positive band around 210 nm obtained for complex relative high concentration is characteristic of a random coil. It differs from β-turn structures; distinguish by a positive CD curve with two picks around 200 and 220 nm.

Thus, according to the observed curves, the protein structures shift from: predominance of α-helix aspect to β-sheet one and finally adopted a random coil structure when the complex rate is relatively important in the medium.

The shift is greater and quicker when the titration of functional unit β_cHlH-g is performed even with concentration 7.5×10^{-5}M of the complex (Fig. 5b) because FU contains only one glycan exposed on the surface of the molecule and the interaction with the complex is easier. The observed shifting in the CD spectra from β-sheet to α-helix structure is another indicator that the carbohydrate chains are located in the so-called β-domain of the functional unit and also explains the conformational changes which occur during the titration process. Native molluscan Hcs result from the oligomerisation of the 11S basic units, forming hollow cylinders where some of the glycans of FUs are buried. Therefore, the native molecule of Hcs is much more stable than the FUs and there is a major hindrance to access the hydrohyl groups of the glycans.

Analysis of the data obtained after the CD measurements are in good correlation with the obtained results by fluorescent measurements.

Conclusion

The carbohydrate structure is very important for the structure and function of hemocyanins and further investigations are needed in this content on the structural and functional role of protein glycosylation. In our previous study we proposed the model that the individual polypeptides of RvH's FUs are linked to each other in a network generated by oligosaccharides [31]. To support this assumption, a complex of pyranine and *o*-BBV (complex) was titrated with Hcs differing in structures and carbohydrate side chains and analysed by fluorescence spectroscopy and circular dichroism. Titration of the complex with different concentrations of native RvH and HlH leads to minimal increase in the fluorescence intensity. During titration with corresponding structural subunits, β_cHlH and RvH2, increase of fluorescence intensity, indicates the availability of more accessible hydroxyl groups than in the native molecules. This experimental data further support our assumption that the hydroxyl groups in the native molecule are buried in the giant quaternary structure, while some of the hydroxyl groups of the structural subunit are located on the surface of the molecule. The titration effect of FUs is even stronger then for the structural subunits and the highest emission was observed after titration of the complex with functional unit βcHlH-g [40] what can be explained by the structutal model of the functional unit βcHlH-g.

The regularities which we have observed in our recent studies, namely low fluorescence changes during titration of native hemocyanins on one side and moderate to strong fluorescence enhancement when titrating with subunits and FUs, additionally support our assumptions that the glycans are involed in the organization of thetrialy structure of molluscan Hcs. One of the function of N-linked oligosaccharide trees may be to organize and stabilize structural subunit of molluscan Hcs.

Acknowledgment This work was financed by research grant № 403 BG051PO001-3.3-05/0001 scheduled "science-business "funded by the Operational Programme" Human Resources", by Bulgarian Ministry of Education, project "Young researchers" DMU 03/26, as well as P. Dolashka and E. Kostadinova thank to German Academic Exchange Service (DAAD) for also supporting this study.

References

1. Martin A, Depoix F, Stohr M, Meissner U, Hagner-Holler S, Hammouti K (2007) *Limulus polyphemus* hemocyanin: 10 Å structure, sequence analysis, molecular modelling and rigid-body fitting reveal the interfaces between the eight hexamers. J Mol Biol 366:1332–1350
2. Del Campo M, Arancibia S, Nova E, Salazar F, González A, Moltedo B, De Ioannes P, Ferreira J, Manubens A, Becker MI (2011) Hemocyanins as immunostimulants. Rev Rev Me Chil 139:236–246
3. Harris JR, Markl J (1999) Keyhole limpet hemocyanin (KLH): a biomedical review. Micron 30:597–623
4. Decker H, Hellmann N, Jaenicke E, Lieb B, Meissner U, Markl J (2007) Minireview: recent progress in hemocyanin research. Integr Comp Biol 47:631–644
5. Gatsogiannis C, Markl J (2009) Keyhole limpet hemocyanin: 9-A CryoEM structure and molecular model of the KLH1 didecamer reveal the interfaces and intricate topology of the 160 functional units. J Mol Biol 385:963–983
6. Meissner U, Dube P, Harris JR, Stark H, Markl J (2000) Structure of a molluscan hemocyanin didecamer (HtH1 from *Haliotis tuberculata*) at 12 A resolution by cryoelectron microscopy. J Mol Biol 298:21–34
7. Schütz J, Dolashka-Angelova P, Abrashev R, Nicolov P, Voelter W (2001) Isolation and spectroscopic characterization of the structural subunits of keyhole limpet hemocyanin. Biochim Biophys Acta 1546:325–336
8. Dolashka-Angelova P, Dolashki A, Savvides S, Hristova R, Van Beeumen J, Voelter W, Devreese B, Weser U, Di Muro P, Salvato B, Stevanovic S (2005) Structure of hemocyanin subunit caeSS2 of the crustacean Mediterranean crab *Carcinus aestuarii*. J Biochem 138:303–312
9. Dolashka-Angelova P, Beltramini M, Dolashki A, Salvato B, Voelter W (2001) Carbohydrate composition of *Carcinus aestuarii* hemocanin. Arch Biochem Biophys 389:153–158
10. Velkova L, Dolashka P, Lieb B, Dolashki A, Voelter W, Van Beeumen J, Devreese B (2011) Glycan structures of the structural subunit (HtH1) of *Haliotis tuberculata* hemocyanin. Glycoconj J 28(6):385–395
11. Dolashka-Angelova P, Velkova L, Shishkov S, Kostova K, Dolashki A, Dimitrov I, Atanasov B, Devreese B, Voelter W, Van Beeumen J (2010) Glycan structures and antiviral effect of the structural subunit RvH2 of Rapana hemocyanin. Carboh Res 345:2361–2367
12. Dolashka-Angelova P, Lieb B, Velkova L, Heilen N, Sandra K, Nikolaeva-Glomb L, Dolashki A, Galabov AS, Beeumen JV, Stevanovic S, Voelter W, Devreese B (2009) Identification of glycosylated sites in Rapana hemocyanin by mass spectrometry and gene sequence, and their antiviral effect. Bioconjug Chem 20:1315–1322
13. Sandra K, Dolashka-Angelova P, Devreese B, Van Beeumen J (2007) New insights in *Rapana venosa* hemocyani N-glycosylation resulting from on-line mass spectrometric analyses. Glycobiology 17:141–156
14. Wood E, Chaplin M, Gielens C, De Sadeleer J, Préaux G, Lontie R (1985) Relative molecular mass of the polypeptide chain of βc-haemocyanin of *Helix pomatia* and carbohydrate composition of the functional units. Comp Biochem Physiol 82:179–186
15. Van Kuik JA, Sijbesma RP, Kamerling JP, Vliegenthart JFG, Wood EJ (1987) Primary structure determination of seven novel N-linked carbohydrate chains derived from hemocyanin of *Lymnaea stagnalis*. Eur J Biochem 169:399–411
16. Wuhrer M, Robijn M, Koeleman C, Balog C, Geyer R, Deelder A, Hokke C (2004) A novel Gal(b1-4)Gal(b1-4)Fuc(a1-6)-core modification attached to the proximal *N*-acetylglucosamine of keyhole limpet haemocyanin (KLH) N-glycans. Biochem J 378:625–632
17. Dolashka P, Velkova L, Iliev I, Beck A, Dolashki A, Yossifova L, Toshkova R, Voelter W, Zacharieva S (2011) Antitumor activity of glycosylated molluscan hemocyanins via guerin ascites tumor. Immunol Investig 40(2):130–149
18. Jurincic-Winkler CD, Metz KA, Beuth J, Klippel KF (2000) Keyhole limpet hemocyanin for carcinoma in situ of the bladder: a long-term follow-up study. Eur Urol 37(3):45–49
19. Jurincic C, Engelmann U, Gasch J, Klippel K (1988) Immunotherapy in bladder cancer with keyhole-limpet hemocyanin: a randomized study. J Urol 139:723–726
20. Riggs DR, Jackson BJ, Vona-Davis L, Nigam A, McFadden DW (2002) In vitro anticancer effects of a novel immunostimulant: keyhole limpet hemocyanin. J Surg Res 108:279–284
21. Riggs DR, Jackson BJ, Vona-Davis L, Nigam A, McFadden DW (2005) In vitro effects of keyhole limpet hemocyanin in breast and pancreatic cancer in regards to cell growth, cytokine production, and apoptosis. The Am J Surg 189:680–684
22. Iliev I, Toshkova R, Dolashka-Angelova P, Yossifova L, Hristova R, Yaneva J, Zacharieva S (2008) Haemocyanins from *Rapana venosa* and *Helix vulgaris* display an antitumour activity via specific activation of spleen lymphocytes. Compt Rend Acad Bulg Sci 61(2):203–210
23. Moltedo B, Faunes F, Haussmann D, Ioannes PD, Ioannes AED, Puente J, Becker MI (2006) Immunotherapeutic effect of concholepas hemocyanin in the murine bladder cancer model: evidence for conserved antitumor properties among hemocyanins. The J Urol 176:2690–2695
24. Toshkova R, Velkova L, Voelter W, Dolashka-Angelova P (2007) Protective effect of Rapana venosa Hemocyanin (RvH) on survivability of hamsters with transplanted myeloid Graffi tumours. C R Acad Bulg Sci 59(9):977–982
25. Toshkova R, Ivanova E, Hristova R, Voelter W, Dolashka-Angelova P (2009) Effect of Rapana venosa hemocyanin on Antibody-Dependent Cell Cytotoxicicity (ADCC) and mitogen responsibility of lymphocytes from hamsters with progressing myeloid tumors. World J Med Sci 4(2):135–142
26. Dolashka-Angelova P, Stevanovic S, Neychev H, Schwarz H, Voelter W (2008) Immunological potential of *Helix vulgaris* and *Rapana venosa* hemocyanins. Immunolog Investig 37(8):822–840
27. Kantele A, Häkkinen MP, Zivny J, Elson CO, Mestecky J, Kantele JM (2011) Humoral immune response to keyhole limpet haemocyanin, the protein carrier in cancer vaccines. Clin Dev Immunol 614383:1–6
28. Miles D, Roché H, Martin M, Perren TJ, Cameron DA, Glaspy J, Dodwell D, Parker J, Mayordomo J, Tres A, Murray JL, Ibrahim NK (2011) Phase III multicenter clinical trial of the sialyl-TN (STn)-keyhole limpet hemocyanin (KLH) vaccine for metastatic breast cancer. Oncologist 16(8):1092–1100
29. Hulíková K, Grobárová V, Křivohlavá R, Fišerová A (2010) Antitumor activity of N-acetyl-D-glucosamine-substituted glycoconjugates and combined therapy with keyhole limpet hemocyanin in B16F10 mouse melanoma model. Folia Microbiol (Praha) 55(5):528–532
30. Dolashka P, Velkova L, Shishkov S, Kostova K, Dolashki A, Dimitrov I, Atanasov B, Devreese B, Voelter W, Van Beeumen J (2010) Glycan structures and antiviral effect of the structural subunit RvH2 of Rapana hemocyanin. J Carbohydr Res 345:2361–2367
31. Dolashka-Angelova P, Stevanovic S, Dolashki A, Devreese B, Tzvetkova B, Voelter W, Beeumen JV, Salvato B (2007) A challenging insight on the structural unit 1 of molluscan *Rapana venosa* hemocyanin. Arch Biochem Biophys 49:50–58

32. Dolashka P, Genov N, Pervanova K, Voelter W, Geiger M, Stoeva S (1996) *Rapana thomasiana* grosse (gastropoda) haemocyanin: spectroscopic studies of the structure in solution and the conformational stability of the native protein and its structural subunits. Biochem J 315:139–144
33. Veklkova L, Dimitrov I, Schwarz H, Stevanovic S, Voelter W, Salvato B, Dolashka-Angelova P (2010) Structure of hemocyanin from garden snail *Helix lucorum*. Comp Biochem Physiol Part B: Biochem Mol Biol 157(1):16–25
34. Arimori S, Ward CJ, James TD (2002) A D-glucose selective fluorescent assay. Tetrahedron Lett 43:303–305
35. Wiskur SL, Ait-Haddou H, Lavigne JJ, Ansyln EV (2001) Teaching old indicators new tricks. Acc Chem Res 34:963–972
36. Arimori S, Murakami H, Takeuchi M, Shinkai S (1995) Sugar-controlled association and photoinduced electron-transfer in boronic-acid-appended porphyrins. J Chem Soc,Chem Commun 961–962
37. DiCesare N, Pinto MR, Schanze KS, Lakowicz JR (2002) Saccharide detection based on the amplified fluorescence quenching of a water-soluble poly(phenylene ethynylene) by a boronic acid functionalized benzyl viologen derivative. Langmuir 18:7785–7787
38. Cappuccio FE, Suri JT, Cordes DB, Wessling RA, Singaram B (2004) Evaluation of pyranine derivatives in boronic acid based saccharide sensing: significance of charge interaction between dye and quencher in solution and hydrogel. J Fluoresc 14:521–533
39. Harris JR, Markl J (2000) Keyhole limpet hemocyanin: molecular structure of a potent marine immunoactivator. Rev Eur Urol 37:24–33
40. GriYoen M, Borghi M, Schrier PI, Osanto S, Schadendorf D (2004) Analysis of T-cell responses in metastatic melanoma patients vaccinated with dendritic cells pulsed with tumor lysates. Cancer Immunol Immunother 53(8):715–722
41. Wang L, Sang YX, Wang XH (2011) Enzyme-linked immunosorbent assay for okadaic acid: investigation of analytical conditions and sample matrix on assay performance. J AOAC Int 94(5):1531–1539
42. Coates CJ, Kelly SM, Nairn J (2011) Possible role of phosphatidylserine-hemocyanin interaction in the innate immune response of *Limulus polyphemus*. Dev Comp Immunol 5(2):155–163
43. Jaenicke E, Fraune S, May S, Irmak P, Augustin R, Meesters C, Decker H, Zimmer M (2009) Is activated hemocyanin instead of phenoloxidase involved in immune response in woodlice. Dev Comp Immunol 33(10):1055–1063
44. Geyer H, Wuhrer M, Resemann A, Geyer R (2005) Identification and characterization of keyhole limpet hemocyanin *N*-Glycans mediating cross-reactivity with *Schistosoma mansoni*. J Biol Chem 280(49):40731–40748
45. Tang BP, Wang YQ, Zhang DZ (2009) Studies on the interaction between benzidine and hemocyanin from Chinese mitten crab *Eriocheir japonica* sinensis (Decapoda, Grapsidae). Spectrochim Acta A Mol Biomol Spectrosc 73(4):676–681
46. Kostadinova E, Dolashka P, Kaloyanova S, Velkova L, Deligeorgiev T, Voelter W, Petkov I (2012) Development of a new method for analysis of different oligosaccharide structures. J Fluoresc 22(6):1609–1615
47. Cuff ME, Miller KI, Van Holde KE, Hendrickson WA (1998) Crystal structure of a functional unit from Octopus hemocyanin. J Mol Biol 278(4):855–870